Blocking Phosphoinositide 3-Kinase Activity in Colorectal Cancer Cells Reduces Proliferation but Does Not Increase Apoptosis Alone or in Combination with Cytotoxic Drugs

Cristina Martin-Fernandez,[1] Juliana Bales,[1] Cassandra Hodgkinson,[1] Arkadiusz Welman,[1] Melanie J. Welham,[2] Caroline Dive,[1] and Christopher J. Morrow[1]

[1]Paterson Institute for Cancer Research, University of Manchester, Manchester, United Kingdom and
[2]Department of Pharmacy and Pharmacology, University of Bath, Bath, United Kingdom

Abstract

In response to growth factors, class IA phosphoinositide 3-kinases (PI3K) phosphorylate phosphatidylinositol-4,5-bisphosphate, converting it to phosphatidylinositol-3,4,5-trisphosphate to activate protein kinase B/Akt. This is widely reported to promote tumorigenesis via increased cell survival, proliferation, migration, and invasion, and many tumor types, including colorectal cancer, exhibit increased PI3K signaling. To investigate the effect of inhibiting PI3K and as an alternative to the use of small molecular inhibitors of PI3K with varying degrees of selectivity, HT29 and HCT116 colorectal cancer cells bearing mutant *PIK3CA* were generated that could be induced with doxycycline to express synchronously a dominant negative subunit of PI3K, Δp85α. On induction, decreased levels of phosphorylated protein kinase B were detected, confirming PI3K signaling impairment. Induction of Δp85α *in vitro* reduced cell number via accumulation in G_0-G_1 phase of the cell cycle in the absence of increased apoptosis. These effects were recapitulated *in vivo*. HT29 cells expressing Δp85α and grown as tumor xenografts had a significantly slower growth rate on administration of doxycycline with reduced Ki67 staining without increased levels of apoptotic tissue biomarkers. Furthermore, *in vitro* Δp85α expression did not sensitize HT29 cells to oxaliplatin- or etoposide-induced apoptosis, irrespective of drug treatment schedule. Further analysis comparing isogenic HCT116 cells with and without mutation in *PIK3CA* showed no effect of the mutation in either proliferative or apoptotic response to PI3K inhibition. These data show in colorectal cancer cells that PI3K inhibition does not provoke apoptosis per se nor enhance oxaliplatin- or etoposide-induced cell death. (Mol Cancer Res 2009;7(6):955–65)

Introduction

The phosphoinositide 3-kinase (PI3K) family of lipid kinases phosphorylate inositol rings on the D3 position (1).

The most thoroughly studied class of PI3K are class IA PI3Ks, which are constitutive heterodimers composed of a catalytic subunit, p110, bound to a regulatory subunit, p85 (2). On receptor tyrosine kinase (RTK) activation, class IA PI3Ks are activated primarily by the recruitment of the p110 subunit to the RTK or RTK-associated adaptor molecules by the p85 subunit via recognition of specific phospho-tyrosine residues. This causes the relocalization of the heterodimer to the plasma membrane (2) in close proximity to its substrate, while potentially also removing allosteric inhibition of p110 by p85 (3, 4). Once activated, the class IA PI3K substrate phosphatidylinositol-4,5-bisphosphate is converted into the secondary messenger phosphatidylinositol-3,4,5-trisphosphate to activate many downstream kinases, most notably protein kinase B (PKB, also known as Akt; ref. 5). The PI3K/PKB signaling network has been reported to promote cell survival, proliferation, and tumor growth, as well as enhance angiogenesis and migration, all important factors in tumorigenesis, suggesting a role for PI3K signaling in cancer (2). Indeed, numerous elements of the PI3K/PKB network are mutated, up-regulated, or down-regulated in several tumor types, all leading to increased PI3K signaling. The most well-studied alteration is the down-regulation or mutation of phosphatase and tensin homologue, the antagonistic phosphatase to class I PI3K, which leads to an increase in the level of phosphatidylinositol-3,4,5-trisphosphate and, consequently, activation of PKB (6, 7). More recently, activating mutations have been discovered in *PIK3CA*, the gene that encodes the class IA catalytic subunit p110α, in numerous cancers including lung cancer, breast cancer, and colorectal cancer (CRC; ref. 8). Furthermore, amplifications in the genes encoding p110α, p85α, and PKB have been described, and there is recent evidence of an activating mutation in PKBα in breast, colorectal, and ovarian cancers (9). In addition to this direct evidence of deregulation of the PI3K/PKB network, it is well documented that RTKs, such as epidermal growth factor receptor, can be aberrantly activated in various cancers, leading to activation of the PI3K/PKB network (10). Indeed, many of the most novel mechanism-based cancer therapeutics, such as gefitinib, cetuximab, and trastuzumab, act through the inhibition of aberrantly activated RTKs, one effect of which will be to reduce signaling through the PI3K/PKB network.

The overwhelming evidence of PI3K/PKB involvement in tumorigenesis means that inhibition of this signaling network is an attractive and tractable avenue of investigation for pharmacologic intervention, and there are several small-molecule inhibitors of PI3Ks that have been developed and historically used as pharmacologic tools with which to study the effect of

PI3K inhibition. The most widely used PI3K inhibitor is LY294002; however, it inhibits other members of the PI3K family (11), as well as non-PI3K family members (12). Wortmannin, another widely used PI3K inhibitor, has a narrower selectivity profile than LY294002, although it also inhibits PLK1 (13). Wortmannin is also unstable in aqueous solutions (14) precluding it from chronic use. More "drug-like" PI3K inhibitors are approaching or entering early clinical trials, although their specificity is only now starting to be reported (12). Therefore, to determine the effect of PI3K inhibition in CRC cells, without the confounding factor of "off-target" effects associated with small-molecule inhibitors, two CRC cell lines with mutant *PIK3CA*, HT29 and HCT116, were engineered to contain an inducible Myc-tagged dominant negative form of the regulatory PI3K subunit p85α, MycΔp85α, which lacks the domain required to interact with catalytic PI3K subunits. These models of inducible and synchronous inhibition of PI3K activity were used to examine the effect of PI3K inhibition on CRC cell survival and proliferation *in vitro* and *in vivo*. The effects of small-molecule inhibitor of PI3K were also compared in isogenic HCT116 CRC cells that had either mutant or wild-type (WT) *PIK3CA* and in SW620 with WT *PIK3CA*. Because PI3K signaling small-molecule inhibitors will most likely be used in combination drug regimens in the clinic, the effect of inhibiting PI3K was also investigated in HT29 cells in combination with oxaliplatin (a DNA-platinating agent that promotes cytostasis in HT29 cells and is routinely used to treat CRC) and with etoposide (a topoisomerase II inhibitor that induces concentration- and time-dependent apoptosis in this cell line).

Results

Generation of HT29 Inducible MycΔp85α Cell Lines

To study the effect of PI3K inhibition in CRC cell lines, a cDNA encoding MycΔp85α, a Myc-tagged version of the bovine regulatory PI3K subunit p85α lacking the internal SH2 domain required for binding to the catalytic p110 subunit, was cloned into the pTRE vector. pTRE contains a disabled cytomegalovirus promoter that is only active in the presence of a tetracycline transactivator protein and tetracycline or its analogues [e.g., doxycycline (dox)]. pTREMycΔp85α was fused with the previously described pN1pβ-actin-rtTA2^S-M2-IRES-EGFP vector, which confers neomycin resistance (15), to generate a single vector, pSMVMycΔp85α. In addition to MycΔp85α, pSMVMycΔp85α encoded the improved tetracycline transactivator protein rtTA2^S-M2 linked via an internal ribosome entry site (IRES) sequence to enhanced green fluorescent protein (EGFP), allowing fluorescence-activated cell sorting of stably transfected clones. pSMVMycΔp85α was electroporated into HT29 cells, which have been characterized extensively with regard to their PI3K signaling pathway (16, 17), are mutant for *PIK3CA* [P449T (18); confirmed by sequencing (data not shown)], and have previously been used to successfully generate inducible cell lines (15). After neomycin selection and cell sorting based on EGFP signal, 48 single HT29 cell clones were generated and screened for the inducible expression of a Myc-tagged protein by Western blotting. Approximately 25% of clones showed robust induction of a Myc-tagged protein at the appropriate size of

~85 kDa; three clones were selected for further evaluation. To confirm that this Myc-tagged protein was indeed MycΔ-p85α parental HT29 cells and HT29 pSMVMycΔp85α clones 12, 15, and 17 (referred to as Δ12, Δ15, and Δ17), cells were grown in the absence or presence of dox for 24 hours, and the resultant cell lysates were assayed by Western blotting for the level of Myc-tagged protein and p85 (Fig. 1A). A Myc-tagged protein was detected only in the presence of dox in all three clones and not detected in the parental cells. Consistent with this Myc-tagged protein being functional MycΔp85α, there was also an increase in the level of p85 in all three clones 24 hours after dox treatment, whereas the level of actin remained constant across all eight samples, indicative of even protein loading. This showed that the addition of dox to the three HT29 pSMVMycΔp85α clones induced the expression of MycΔp85α; however, it was noticeable that the level of expression varied between the three clones, with clone Δ15 expressing the greatest amount of MycΔp85α. Therefore, to determine whether this was due to heterogeneity within cell populations, where some of the cells do not express MycΔp85α, or whether there were different expression levels between the clones, immunohistochemistry was carried out with an anti–Myc-tag antibody (Fig. 1B). This showed that in each clone, all the cells expressed a Myc-tagged protein, whereas clone Δ15 exhibited the strongest staining intensity. Thus, the differences in MycΔp85α levels observed in cell lysates were due to different expression levels between the three clones.

Expression of MycΔp85α Inhibited PI3K Signaling

To determine whether expression of MycΔp85α led to the inhibition of PI3K signaling, cells were treated with dox for 24 hours and phosphorylation status of downstream targets of the PI3K pathway was assessed by Western blotting. Whereas the addition of dox to parental cells had no effect on phosphorylation of Ser473 of PKB (Fig. 1C), the expression of MycΔ-p85α promoted down-regulation of PKB phosphorylation in all three clones. However, it seemed there was greater down-regulation of PKB phosphorylation in clone Δ15 than in the other clones, consistent with the observation of increased induction of MycΔp85α in this clone. Taken together, these data showed that expression of MycΔp85α leads to inhibition of PI3K signaling in HT29 cells.

Expression of MycΔp85α Reduced Proliferation but Did Not Provoke Apoptosis In vitro

The effect of MycΔp85α expression on cell population growth kinetics was investigated to explore whether MycΔp85α expression modulated cell cycle progression and/or cell death. Cells were left untreated or treated with dox on day 0 and the increase in cell number (as measured by protein stain) with time was calculated relative to day 0. All of the clonal cell populations increased at the same rate as the parental cell line in the absence of dox, and dox did not affect the population growth rate of the parental cell line (Fig. 2A). In the presence of dox, cell numbers of all clonal populations increased more slowly than seen in the absence of dox, with a significant reduction in cell population observed as early as day 2. To determine the underlying mechanism of the MycΔp85α-mediated reduction in cell population, the cell cycle profile was analyzed for untreated cells and cells that had been treated with dox for 24 hours. The DNA profiles of

the three clones in the absence of dox were the same as parental cells, and dox had no effect on the DNA profile of parental cells. The effect of MycΔp85α expression was to significantly increase the proportion of cells in the G_0-G_1
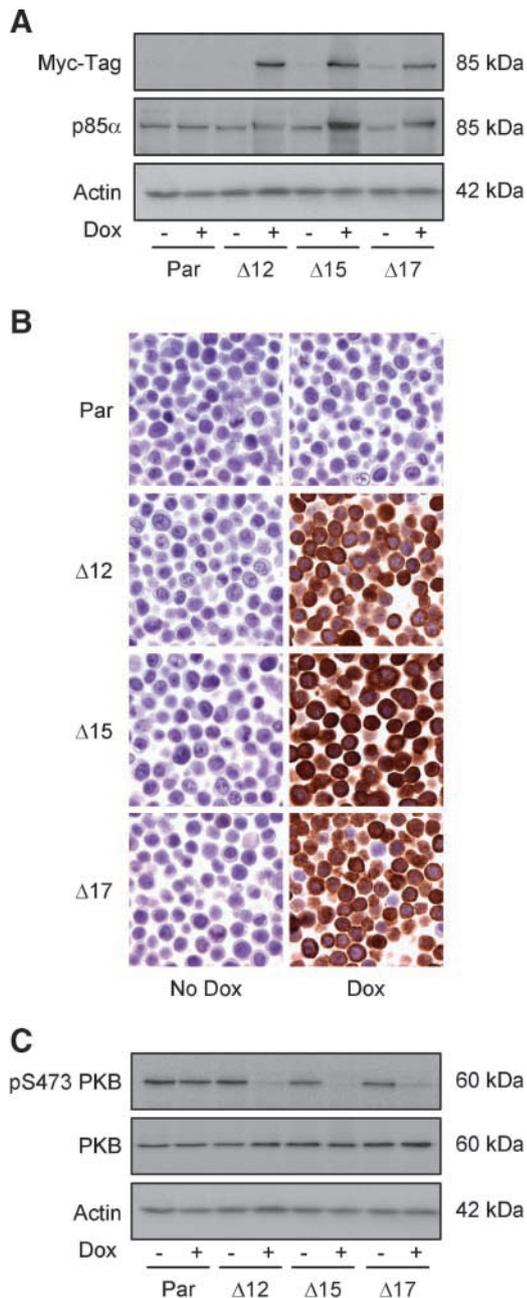
FIGURE 1. Inducible expression of MycΔp85α inhibits PI3K activity. Parental HT29 cells (*Par*) or clones 12, 15, and 17 containing pSMVMycΔ-p85α (*Δ12, Δ15,* and *Δ17*) were grown in the absence (– or *No Dox*) or presence (+ or *Dox*) of 0.5 mg mL^{-1} dox for 24 h and either lysed for Western blot analysis (**A** and **C**) or fixed with 10% formalin (**B**). **A.** Cell lysates were assayed for the expression of Myc-tagged proteins, p85, and actin (loading control) by Western blotting. **B.** Formalin-fixed cells were analyzed for the expression of Myc-tagged protein by immunohistochemistry analysis. **C.** Cell lysates were assayed for the level of PKB phosphorylated on serine residue 473 (*pS473 PKB*), total PKB, and actin (loading control). Representative images from at least three independent experiments.

phase of the cell cycle (Fig. 2B, *top*), with a corresponding decrease of cells in S phase and G_2-M phase (data not shown). This suggested that the reduction in cell number observed in cells with impaired PI3K signaling was due, at least in part, to reduced proliferation associated with a delay in cell cycle progression.

One mechanism whereby PI3K inhibition could lead to a G_1 arrest would be by the enhanced expression of the cyclin-dependent kinase inhibitor p27, which is translated in a FKHR-dependent manner, inhibitable by PI3K activity (19). p27 expression was assessed in lysates from parental cells and clones treated with dox for 24 hours. Whereas the addition of dox to parental cells had no effect on p27 expression level, the induction of MycΔp85α led to a marked increase in p27 level (Fig. 2, *bottom*). Therefore, PI3K inhibition in HT29 cells leads to a G_1 delay, consistent with increased expression of p27. However, whereas cell cycle delay contributed to the reduction in cell number, it remained possible that inhibition of PI3K might also have promoted cell death. Moreover, because PI3K activity has been widely reported to have prosurvival affects (2), the effect of MycΔp85α expression on apoptosis was investigated.

Cell cycle profiles had not indicated any increase in cells with an apoptotic sub-G_1 DNA content regardless of dox addition, suggesting that MycΔp85α expression did not cause apoptosis (data not shown). To more thoroughly test this observation, MycΔp85α-expressing cells were analyzed using two different methods to detect apoptosis. Untreated and 24-hour dox-treated cells were analyzed by flow cytometry for phosphatidylserine exposure and 7-amino-actinomycin D (7-AAD) exclusion using 100 μmol/L etoposide–treated parental HT29 cells as a positive control. In parental cells, the level of nonpermeable cells with exposed phosphatidylserine (Annexin V positive/7-AAD negative, indicative of apoptosis; Fig. 2C) and that of permeable cells (Annexin V positive/7-AAD positive, indicative of primary or secondary necrosis; data not shown) were negligible, regardless of dox treatment, whereas etoposide treatment caused a significant increase in both subpopulations. MycΔp85α expression had no significant effect on the amount of nonpermeable/Annexin V–positive cells or permeable cells although there was a trend to suggest that MycΔp85α expression might have increased the number of nonpermeable/Annexin V–positive cells from 0.8% to 1.6%, especially in clone Δ15. This result was verified by examining the level of cleaved caspase-3 in cell lysates after 24 hours of dox treatment using a duplex ELISA-based assay that detects both cleaved and total caspase-3. Caspase-3 cleavage was not induced in parental cells by dox treatment, whereas etoposide treatment significantly increased the level of caspase-3 cleavage (Fig. 2D). MycΔp85α expression did not cause a significant level of caspase-3 cleavage in any of the clones, although again there is a slight (1%) increase in clone Δ15. Taken together, these data suggest that PI3K inhibition for 24 hours did not induce a significant level of apoptosis per se in HT29 cells.

MycΔp85α Induction in HCT116 CRC Cells Also Caused Cell Cycle Arrest

To determine whether the effect of MycΔp85α induction in HT29 cells also occurred in another CRC cell line, clones

containing pSMVMycΔp85α were generated in HCT116. Like HT29 cells, HCT116 cells contain a mutant *PIK3CA* (H1047R; ref. 20, 21). Data presented here are for HCT116 MycΔp85α clone 23 (Δ23), but similar data have also been obtained from another two clones (data not shown). Initially, the dox-inducible expression of MycΔp85α was tested by Western blotting for levels of Myc-tagged protein and p85 in lysates from parental and Δ23 cells grown in the presence or absence of dox for 24 hours (Fig. 3A, *top two rows*). HCT116 lysates contained an unrelated 85-kDa protein, which was detected by the Myc-tag antibody observed in both parental and Δ23 cell lysates; however, there is a clear increase in the intensity of a band at 85 kDa on addition of dox to Δ23

cells. Furthermore, there is increased expression of protein detected by p85 antibodies, which migrates slightly more slowly than endogenous p85α in dox-treated Δ23 lysates. This showed that MycΔp85α is induced on addition of dox to Δ23 cells. To determine whether MycΔp85α expression also impaired PI3K signaling, the level of phospho-PKB in the same lysates was investigated (Fig. 3A, *bottom two rows*). The addition of dox to parental HCT116 cells had no effect on the level of PKB-phosphorylation, whereas the addition of dox to Δ23 cells caused a clear decrease in phospho-PKB, consistent with MycΔp85α expression inhibiting PI3K activity. The HCT116 cell population growth kinetics was assessed, using the sulforhodamine B (SRB) assay, for the
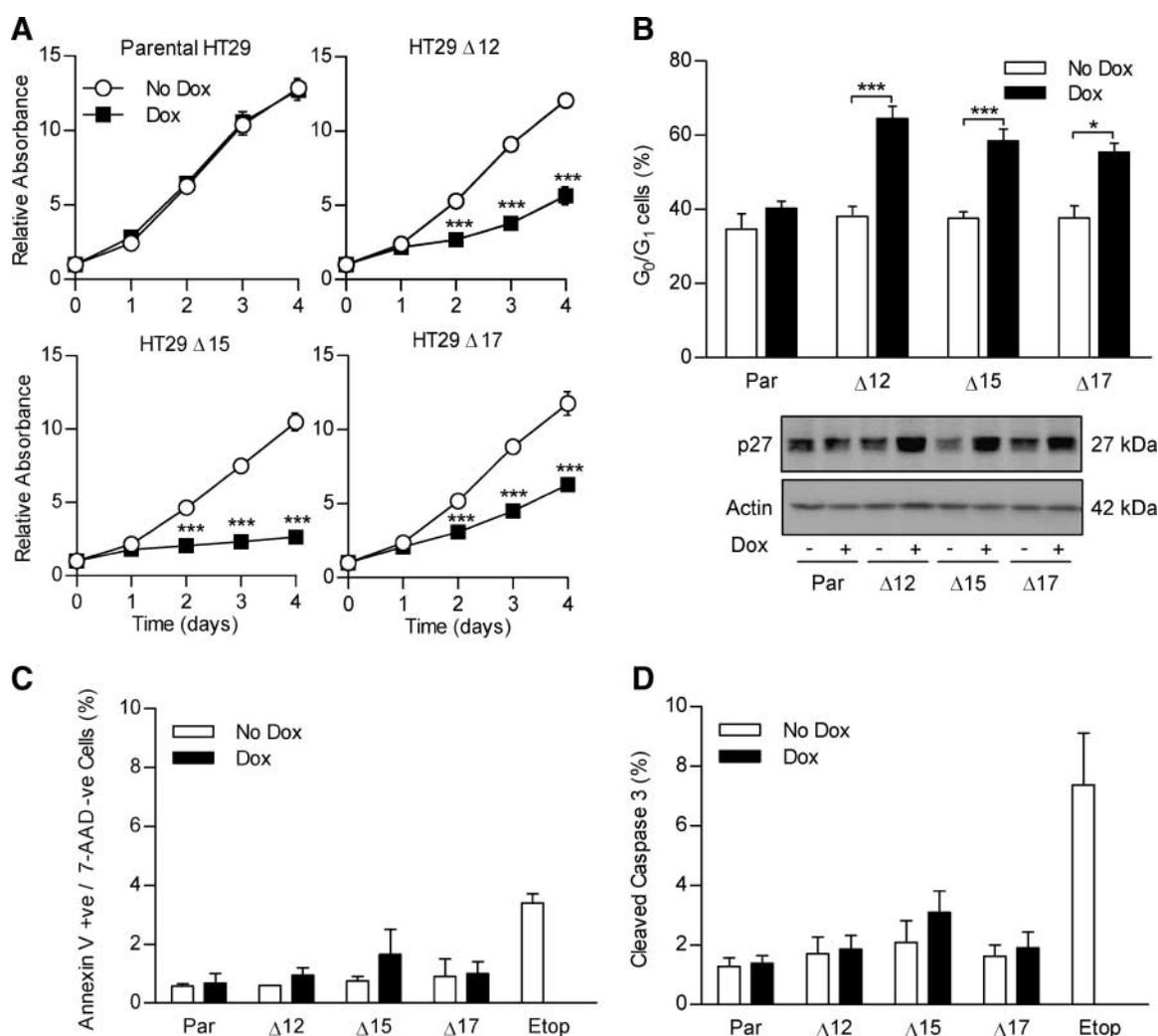
FIGURE 2. MycΔp85α expression prevents cell proliferation by causing a G_0-G_1 arrest without inducing apoptosis *in vitro*. **A.** Cells were seeded into 96-well plates and, after 24 h, treated with 0.5 mg mL^{-1} dox or left untreated. A plate was harvested every 24 h for 4 d and the amount of protein in each well relative to day 0 was determined by SRB staining. **B.** Cells were grown in the absence or presence of dox for 24 h and harvested by trypsinization and fixed in 70% ethanol. Cells were then stained with propidium iodide, and the amount of propidium iodide incorporated into cells was determined by flow cytometry. The percentage of cells in the G_0-G_1 stage of the cell cycle was then calculated using Modfit LT 3.2 software. **C.** Cells grown in the absence or presence of dox for 24 h were harvested by trypsinization and stained with Annexin V and 7-AAD. Samples were analyzed by flow cytometry and the percentage of Annexin V–positive, 7-AAD–negative cells was calculated. **D.** Cells were grown in the presence or absence of dox for 24 h and lysed. Lysate containing 20 µg of total protein was analyzed in duplicate on Mesoscale Discovery cleaved caspase-3 and total caspase-3 duplex plates, and the percentage of cleaved caspase-3 determined. All graphs represent the mean from three independent experiments; bars, SE. *, $P < 0.05$; **, $P < 0.01$; ***, $P < 0.001$, compared with the corresponding no dox treatment (two-tailed unpaired t test). Blots are representative of three independent experiments.
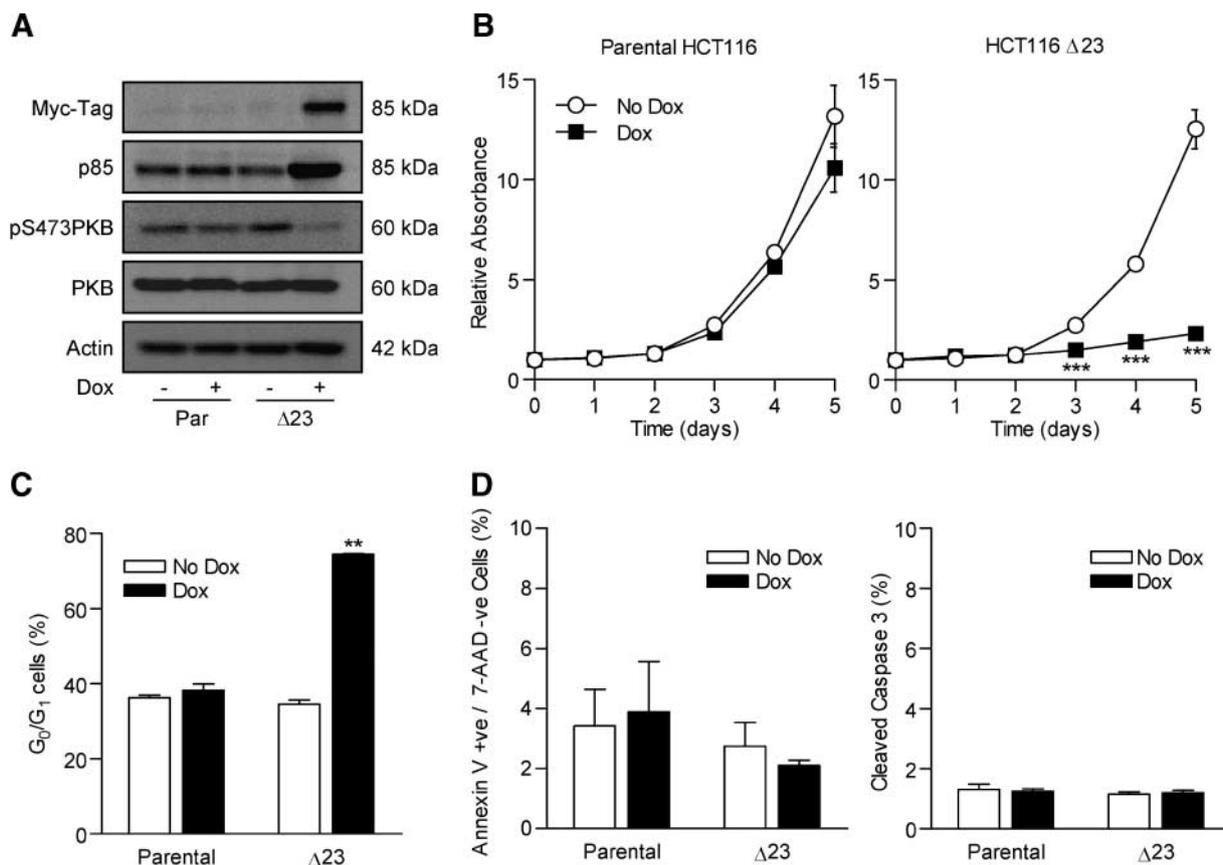
FIGURE 3. MycΔp85α expression inhibits PI3K signaling and causes a cell cycle arrest in HCT116 cells. **A.** Parental HCT116 and clone Δ23 cells were grown in the presence or absence of 0.5 mg mL^{-1} dox for 24 h and lysed. Lysates were assayed for the levels of Myc-tagged protein, p85, phospho-PKB, and total PKB by Western blotting. **B.** Cells were seeded into 96-well plates and, after 24 h, treated with 0.5 mg mL^{-1} dox or left untreated. A plate was harvested every 24 h for 5 d and the amount of protein in each well relative to day 0 was determined by SRB staining. ***, $P < 0.001$, compared with the corresponding no dox treatment (two-tailed unpaired t test). **C.** Cells were grown in the absence or presence of dox for 24 h and harvested by trypsinization and fixed in 70% ethanol. The cell cycle profile was determined, and the percentage of cells in the G_0-G_1 stage of the cell cycle calculated as in the previous figure. **, $P < 0.01$, compared with all other groups (two-tailed unpaired t test). **D.** Cells were grown in the absence or presence of dox for 24 h. The percentage of Annexin V–positive/7-AAD–negative cells and the percentage of cleaved caspase-3 were determined as in the previous figure. All graphs represent the mean from three independent experiments; bars, SE. Blots are representative of three independent experiments.

effect of MycΔp85α expression, and it was significantly reduced in Δ23 cells in the presence of dox compared with all other groups (Fig. 3B). This reduction in population growth kinetics correlated with a cell cycle delay, as shown by an increase in Δ23 cells in the G_0-G_1 stage of the cell cycle after MycΔp85α induction (Fig. 3C). Furthermore, MycΔp85α expression did not cause apoptosis, as assessed by Annexin V/7-AAD assay and the level of cleaved caspase-3 (Fig. 3D). This suggested that in HCT116 cells, inhibition of PI3K activity led to a reduction in cell proliferation that was caused by cell cycle delay and not apoptosis, as seen in HT29 cells. These results were phenocopied with the relatively specific PI3K small-molecule inhibitor PI-103 (Fig. 4, described below), consistent with PI3K inhibition, and not simply an artifact of protein overexpression.

PI3K Inhibition–Mediated Cytostasis Was Not Dependent on PIK3CA Mutation

The data described above pertained to cell lines that are mutant for *PIK3CA*. Therefore, to determine whether the cytostatic effect of PI3K inhibition occurring without apoptosis was dependent on *PIK3CA* mutation, the effect of inhibiting PI3K activity was compared between SW620 cells, which are WT for *PIK3CA* (18), and HCT116 cells. Moreover, as a more stringent test, the response to PI3K inhibition of isogenic HCT116 cells expressing only WT or mutant *PIK3CA* was compared; this was achieved through targeted insertion of a disruptive DNA sequence at the start of either the WT or mutant allele (21).

HCT116 and SW620 cells treated with 1 μmol/L PI-103 for 24 hours, and the levels of phospho-PKB and total PKB, the cell cycle profile, and the level of apoptosis were analyzed. In both cell lines, PI-103 treatment caused a reduction in the levels of phospho-PKB, without affecting the levels of PKB (Fig. 4A, *left*). It is, however, interesting to note that a higher level of phospho-PKB was observed in HCT116 cells (mutant *PIK3CA*) than in SW620 cells (WT *PIK3CA*). Cell cycle analysis revealed that inhibition of PI3K signaling was associated with a significant increase in the number of cells with a 2n DNA content in both cell lines (Fig. 4B), consistent with a G_0-G_1 cell cycle arrest. The percentage of cells with a 2n

DNA content in the absence of PI-103 was significantly lower in HCT116 cells than in SW620 cells, suggesting that HCT116 cells spend less time in G_1 stage of the cell cycle than SW620 cells, consistent with their increased level of phospho-PKB. PI-103 treatment had no effect on apoptosis in either HCT116 or SW620 cells, as assessed by apoptotic morphology (Fig. 4C) and cleaved caspase-3 (Fig. 4D).

Whereas SW620 cells are *PIK3CA* WT, they carry a *KRAS* mutation (18), which may activate PI3K signaling. As previously described (21), Fig. 4A (*right*) shows that HCT116 cells expressing only mutant *PIK3CA* have higher levels of phosphorylated PKB than those expressing only WT *PIK3CA*, but in both cases, 1 μmol/L PI-103 reduced the level of phospho-PKB. PI-103 treatment caused G_0-G_1 arrest in both mutant and WT *PIK3CA* HCT116 cells (Fig. 4B). Furthermore, PI-103 treatment did not cause apoptosis in either cell line (Fig. 4C and D). Taken together, these data suggest that the effect of PI3K inhibition (by small-molecule inhibitor or induction of dominant negative p85α) seen in HT29 and HCT116 cells is not specific to CRC cells that contain a mutation in *PIK3CA*.

MycΔp85α Expression Was Induced In vivo, Leading to Reduced Tumor Growth without Increased Apoptosis

To determine whether the inhibition of cell proliferation and the lack of apoptosis caused by the induction of MycΔp85α were recapitulated under more physiologic conditions, clone Δ15 and parental HT29 cells were grown as s.c. tumor xenografts in nude mice. Once the tumors reached 300 mm³, mice were fed with either dox-impregnated feed or control feed. To confirm that dox feed induced the expression of MycΔp85α in clone Δ15 xenografts, mice were sacrificed 3 days after being switched to dox or control feed, and the presence of Myc-tagged protein expression in the xenografts was determined by immunohistochemistry and Western blotting (Fig. 5A). Exogenous Myc-tagged protein was detected in Δ15 xenografts when the tumor-bearing animal had been fed with dox feed, and not in any other xenografts. The cells in the xenografts that did not stain with the anti–Myc-tag antibody had a fibroblast-like morphology and are therefore likely to be murine tumor stroma that should not express MycΔp85α, as opposed to HT29 cells that had not induced MycΔp85α. The effect of MycΔp85α expression *in vivo* on tumor growth was investigated by measuring the
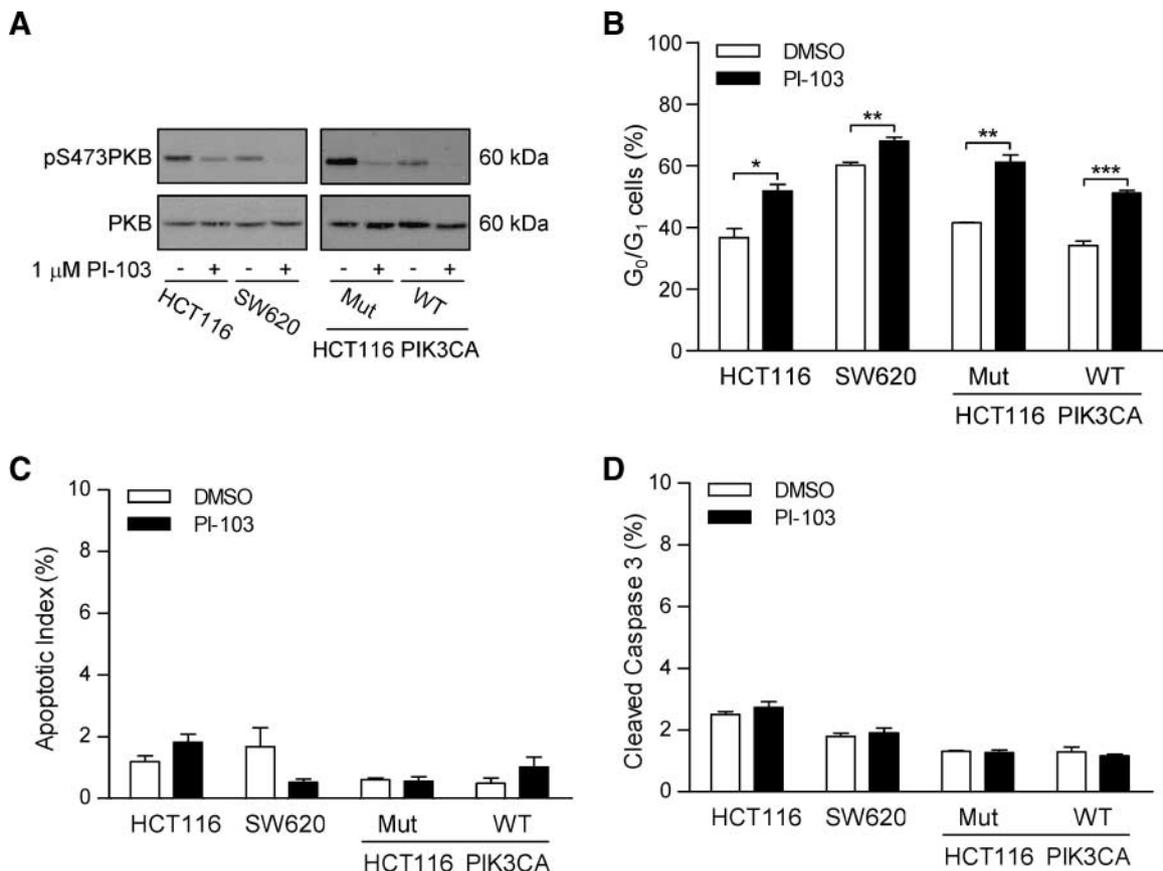
FIGURE 4. PI3K inhibition causes cell cycle arrest, but not apoptosis, in PIK3CA WT cells. HCT116 and SW620 cells (*left*) or HCT116 *PIK3CA* mutant (*Mut*) or WT cells (*right*) were grown in the absence or presence of 1 μmol/L PI-103 for 24 h. Cells were lysed or fixed in 70% ethanol. **A.** Lysates were assayed for the levels of phospho-PKB and total PKB. **B.** The cell cycle profile was determined, and the percentage of cells in the G_0-G_1 stage of the cell cycle calculated as in previous figures. **C.** Fixed cells were stained with DAPI and the percentage of nuclei with an apoptotic morphology was counted. **D.** The percentage of cleaved caspase-3 in lysates was determined as in previous figures. Blots are representative of two independent experiments. Graphs represent the mean from three independent experiments; bars, SE. *, $P < 0.05$; **, $P < 0.01$; ***, $P < 0.001$ (two-tailed unpaired t test).
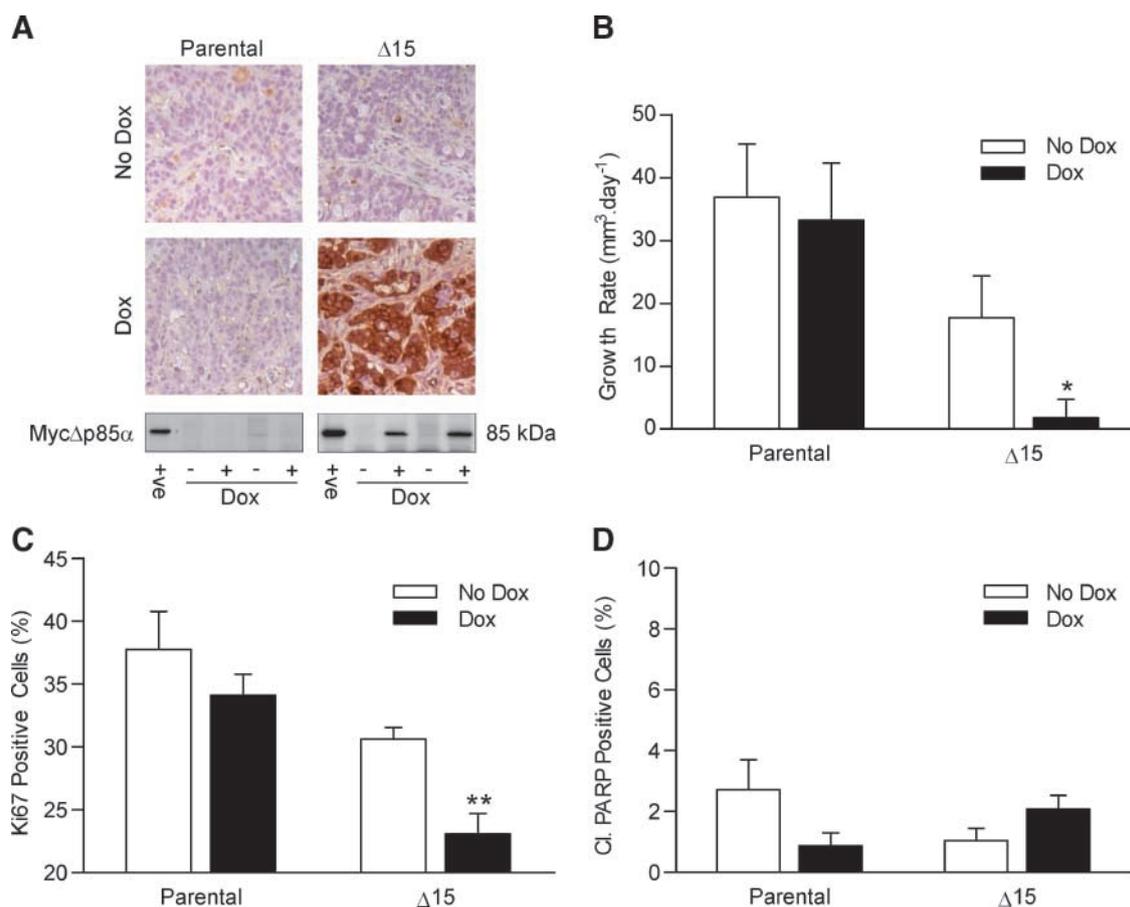
FIGURE 5. MycΔp85α expression inhibits xenografts tumor growth rate and Ki67 staining but has no effect on the level of PARP cleavage. Parental HT29 cells and clone Δ15 cells were grown as tumor xenografts on BALB/c-nude mice and tumors were measured three times a week by calipers. Once tumors reached 300 mm³, mice were switched to feed containing dox or control feed. Four animals were sacrificed 3 d after being switched to dox or control feed and their tumors were bisected and either snap frozen or fixed in 10% formalin. A further six mice from each group were used for tumor growth analysis. **A.** Top, tumors were assayed for the presence of Myc-tagged proteins by immunohistochemistry. Bottom, tumor lysates were assayed for the presence of MycΔp85α by Western blotting. +ve, positive control of a dox-induced clone Δ15 cell lysate. **B.** Columns, mean tumor growth rate from each group of mice after the tumor reached 300 mm³; bars, SE. **C** and **D.** Tumors were stained for Ki67 (**C**) and cleaved PARP (**D**) by immunohistochemistry and the percentage of positive cells was counted. Columns, mean; bars, SE. *, $P < 0.05$; **, $P < 0.01$, compared with all other groups (two-tailed unpaired t test).

volume of the tumors every 2 to 3 days (Fig. 5B). The tumor xenografts derived from parental cells grew by 37 and 33 mm³ d⁻¹ on animals fed with control or dox-laced feed, respectively (no significant difference). The growth rate of Δ15 xenografts grown on animals fed with control feed was 17 mm³ d⁻¹ (not significantly different from parental cells). However, the growth rate of Δ15 dox-fed xenografts was reduced to 2 mm³ d⁻¹ ($P < 0.05$, versus all other conditions), showing that expression of MycΔp85α reduced the growth rate of HT29 xenografts. As was the case *in vitro*, the reduced HT29 tumor growth rate could be due to reduced cell proliferation and/or increased apoptosis. Therefore, xenografts harvested after 3 days of control or dox feed were stained for the proliferation marker Ki67 (Fig. 5C) or cleaved poly(ADP-ribose) polymerase (PARP), which is indicative of apoptosis (Fig. 5D). The number of Ki67-positive cells was not significantly different between parental xenografts from animals fed with control or dox feed or Δ15 xenografts fed with control feed (38%, 34%, and 31%, respectively). However, the number of Ki67-positive cells was significantly less in Δ15 xenografts of mice on dox feed

(23%; $P < 0.01$, versus all other conditions), suggesting that the reduction in tumor growth was, at least in part, due to reduced cell proliferation. There were no significant differences between the four groups of mice with respect to the level of cleaved PARP (Fig. 5D), whereas there is a suggestion of more cleaved PARP–positive cells in the Δ15 dox-treated xenografts than the untreated xenografts; this was within the normal variation for this assay (as shown by the difference between the untreated and dox-treated parental xenografts). Taken overall, the data show that induced MycΔp85α expression did not provoke apoptosis in HT29 xenografts, consistent with the lack of Δ15 xenograft regression after animals were switched to dox feed and with the *in vitro* findings.

PI3K Inhibition Did Not Enhance Oxaliplatin-Induced Apoptosis

If PI3K inhibitors were to be approved for use in the clinic for the treatment of CRC, current practice would suggest that they would be used in combination with the best available treatment. One of the drugs most commonly used to treat CRC is

oxaliplatin, whose main mechanism of action is thought to be DNA damage through the formation of DNA-platinum adducts (22). Whereas expression of MycΔp85α did not enhance apoptosis per se in HT29 cells grown *in vitro* or *in vivo*, it is possible that it primes for drug-induced apoptosis by reducing the threshold at which apoptosis can be engaged. Therefore, cells were treated with a concentration of oxaliplatin that caused between 5% and 10% apoptosis after a 48-hour constant challenge (10 μmol/L for parental, Δ12, and Δ17 cells; 3 μmol/L for

Δ15 cells) or an equivalent vehicle control, and MycΔp85α expression was either not induced (*no dox*) or induced 24 hours before the addition of oxaliplatin (*dox 1st*), at the same time as oxaliplatin (*tog*), or 24 hours after oxaliplatin (*ox 1st*). The apoptotic index was determined by staining nuclei with 4′,6-diamidino-2-phenylindole (DAPI) and counting the percent nuclei with a classic apoptotic morphology. For all four cell lines, parental, Δ12, Δ15, and Δ17, oxaliplatin treatment caused a significant increase in the number of apoptotic cells in the absence of dox (Fig. 6A). As expected, in the parental cells, the addition of dox did not affect the levels of apoptosis induced by oxaliplatin treatment. Furthermore, with the exception of clone Δ15, the expression of MycΔp85α did not affect the level of apoptosis, irrespective of when it was induced relative to the oxaliplatin treatment. For clone Δ15, induction of MycΔp85α before oxaliplatin treatment reduced oxaliplatin-induced apoptosis, whereas the addition of dox at the same time as or after oxaliplatin had no effect on the levels of apoptosis. This could be due to the higher level of MycΔp85α expression in clone Δ15 (relative to the other clones) and that PI3K inhibition is more pronounced in this clone, or it could be due to other clonal variations. In either case, inhibition of class IA PI3K signaling in HT29 cells did not enhance oxaliplatin-induced apoptosis. To confirm this observation, the level of caspase-3 cleavage in cells treated in the same way was determined using the Meso Scale Discovery ELISA–based system (Fig. 6B). In the absence of dox, oxaliplatin treatment caused a significant increase in the level of cleaved caspase-3 (relative to total caspase-3). The addition of dox to parental cells had no effect on the levels of apoptosis, and the induction of MycΔp85α did not change the levels of oxaliplatin-induced caspase-3 cleavage relative to no dox in any clones for any schedule. These data show that PI3K inhibition did not enhance oxaliplatin-induced apoptosis in HT29 cells.

PI3K Inhibition Did Not Enhance Etoposide-Induced Apoptosis

Although oxaliplatin can induce apoptosis when used at high concentrations, it is primarily thought to act as a cytostatic agent at concentrations achieved in the clinic (23). Therefore, the effect of MycΔp85α induction on the apoptotic response of a cytotoxic drug, etoposide, which is associated with apoptotic
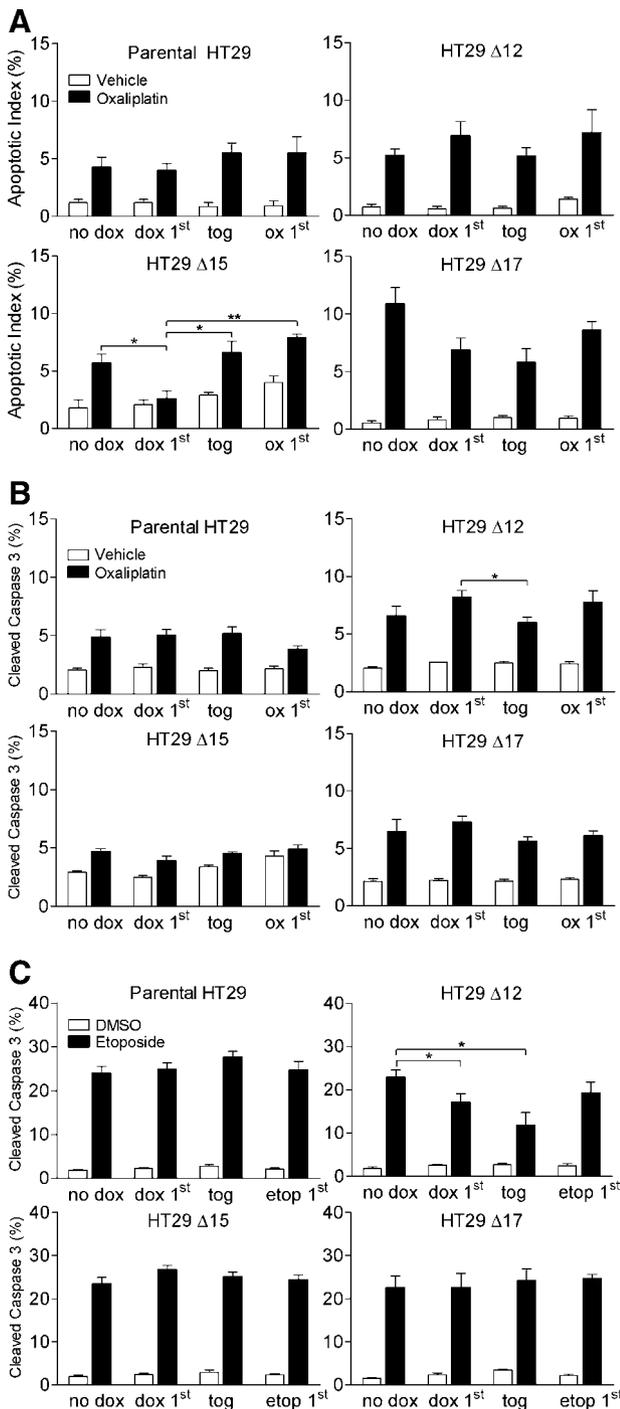
FIGURE 6. MycΔp85α expression does not enhance oxaliplatin-induced or etoposide-induced apoptosis. **A** and **B.** Cells were treated for 48 h with a concentration of oxaliplatin that gave 5% to 10% apoptosis or with vehicle control (PBS). Either this was the only treatment the cells received (*no dox*) or the cells were also treated with dox 24 h before oxaliplatin (*dox 1st*), at the same time as oxaliplatin (*tog*), or 24 h after oxaliplatin (*ox 1st*). Forty-eight hours after the start of oxaliplatin treatment, cells were harvested by trypsinization and either fixed in 70% ethanol or lysed. **A.** Fixed cells were stained with DAPI, and the percentage of cells with an apoptotic nuclei was counted. **B.** The percentage of cleaved caspase-3 within lysates was determined as described in previous figures. **C.** Cells were treated for 48 h with 100 μmol/L etoposide or DMSO equivalent. Either this was the only treatment the cells received (*no dox*) or the cells were also treated with dox 24 h before etoposide (*dox 1st*), at the same time as etoposide (*tog*), or 24 h after etoposide (*etop 1st*). Forty-eight hours after the start of etoposide treatment, cells were harvested by trypsinization and lysed. The percentage of cleaved caspase-3 within lysates was determined using Mesoscale Discovery cleaved caspase-3 and total caspase-3 duplex plates. Columns, mean from three independent experiments; bars, SE. *, $P < 0.05$; **, $P < 0.01$ (two-tailed unpaired t test).

responses *in vitro* and *in vivo*, was explored using the caspase-3 and cleaved caspase-3 ELISA. Cells were treated for 48 hours with etoposide, and MycΔp85α expression was either not induced (*no dox*) or induced 24 hours before (*dox 1st*), at the same time as (*tog*), or 24 hours after (*etop 1st*) the start of etoposide treatment. Etoposide treatment (100 μmol/L) in parental cells, clone Δ15, and clone Δ17 led to ~20% cleaved caspase-3, and this level was not affected by the addition of dox, irrespective of the schedule (Fig. 6C). In clone Δ12, etoposide treatment in the absence of dox also led to ~20% cleaved caspase-3; however, MycΔp85α expression induced before or at the same time as etoposide treatment led to a significant decrease in the level of cleaved caspase-3. It seems unlikely that this represents a bona fide inhibition of etoposide-induced apoptosis by PI3K inhibition because it only occurs in one clone and is therefore more likely due to clonal variation. However, what these data show is that PI3K inhibition did not enhance etoposide-induced apoptosis in HT29 CRC cells.

Discussion

This study has shown that inhibition of PI3K signaling in HT29 and HCT116 CRC cell lines by inducible overexpression of a dominant negative isoform of the regulatory PI3K subunit p85α leads to cell cycle delay in the G_0-G_1 phase of the cell cycle without apoptosis *in vitro*. Furthermore, inhibition of PI3K with the small-molecule inhibitor PI-103 gave a similar effect in CRC cell lines with mutant or WT *PIK3CA*. Consistent with these data, induced expression of MycΔp85α in HT29 xenografts led to a reduction in tumor growth rate, a reduction in Ki67-positive cells, and no change tumor apoptosis. In addition, MycΔp85α expression in HT29 cells did not enhance oxaliplatin- or etoposide-induced apoptosis regardless of whether MycΔp85α was induced before, at the same time, or after the start of drug treatment.

The rationale for studying PI3K inhibition in CRC cells using models that allowed the inducible expression of a dominant-negative PI3K isoform was threefold. First, using a genetic system rather than small-molecule inhibitors to inhibit PI3K allowed for a greater degree of confidence that any results were due to inhibition of PI3K activity, as opposed to off-target effects of any small-molecule inhibitor. Second, the inducible expression of MycΔp85α allowed the study of cells immediately after inhibition of PI3K activity, whereas stable constitutive overexpression would only allow the study of PI3K inhibition weeks to months after PI3K inhibition has been initiated after the appropriate clones had been selected and screened. Finally, all the commercially available PI3K inhibitors are problematic for *in vivo* studies due to poor pharmacokinetic profiles, whereas the pharmacokinetics of dox was not a hindrance to robust induction of MycΔp85α *in vivo*.

The main effect of PI3K inhibition in both HT29 and HCT116 cells was the accumulation of cells with 2n DNA content and accumulation of p27, suggesting G_0-G_1 arrest. This was somewhat to be expected because treatment of a variety of cell lines with various different PI3K small-molecule inhibitors has been reported to induce a G_0-G_1 arrest (24-26). What is perhaps more surprising is that inhibition of PI3K signaling, which is commonly associated with cell survival signaling,

did not increase apoptosis, although a similar lack of apoptosis but reduction of cell proliferation has been reported with PI3K signaling inhibition in hematopoietic cells (27). However, the majority of research implicating PI3K signaling with apoptosis has been carried out with the small-molecule inhibitor LY294002, which, as well as potently inhibiting PI3K activity, also inhibits many other members of the PI3K superfamily as well as casein kinase 2 (28). Furthermore, LY294002 can lead to an increase in intracellular H_2O_2 in prostate, leukemic, and bladder cancer cell lines via a PI3K-independent mechanism, enhancing drug-induced apoptosis (29). Therefore, the expectation that PI3K inhibition should drive apoptosis per se may be an oversimplification. Indeed, recent work with a more selective PI3K inhibitor, PI-103, in a range of cell lines failed to detect apoptosis at PI-103 concentrations that clearly inhibited PI3K activity (25), consistent with the findings reported here.

Whereas it could be argued that PI3K inhibition does not cause apoptosis *in vitro* because the cells are grown under non-physiologic conditions, in the presence of 10% fetal bovine serum and normal oxygen levels, this is not the case *in vivo*, where there are reduced levels of growth or survival factors and oxygen tension due to irregular tumor xenograft vasculature. Indeed, even under these more stringent conditions, no evidence could be found that PI3K inhibition causes apoptosis, whereas a reduction in tumor growth and proliferation was readily detected.

The hypothesis that PI3K inhibition could reduce the threshold for apoptosis was tested using two different drugs, oxaliplatin and etoposide, and in neither case did PI3K inhibition lead to enhanced levels of apoptosis. Because MycΔp85α expression caused a cell cycle delay and drug-induced apoptosis is often cell cycle dependent, different schedules of PI3K inhibition and drug treatment were evaluated but no schedules led to enhanced apoptosis. Of interest and possible clinical benefit, PI3K inhibition before oxaliplatin treatment did not reduce the levels of oxaliplatin- or etoposide-induced apoptosis as might have been predicted for an agent reported to require proliferation for cytotoxicity.

This study does not rule out the possibility that PI3K inhibition could enhance apoptosis in other cell contexts or that induced by other chemotherapeutics or novel kinase inhibitors that are now entering the clinic.

Whereas PI3K inhibition did not seem to affect apoptosis in HT29 or HCT116 cells, the reduction in proliferation that was observed is encouraging. Many current therapeutics have cytostatic properties, and the almost total inhibition of cell proliferation and tumor growth seen both *in vitro* and *in vivo* suggests that PI3K inhibition may be beneficial in the clinic.

PI3K inhibition also caused cell cycle arrest in CRC cells (SW620 and HCT116) that did not contain a *PIK3CA* mutation (Fig. 4) but were mutant for *KRAS* (18), one effect of which is likely to be activation of the PI3K pathway (30). The loss of phosphatase and tensin homologue is a further mechanism observed in CRC cells to activate PI3K signaling (31). This may lead one to speculate that PI3K inhibition might be a valuable cytostatic therapy in the majority of CRC cancers, and perhaps in other cancer types such as glioblastoma (32), where aberrations in the PI3K signaling pathway are common.

Finally, these inducible cell lines are being exploited as useful tools to develop imaging biomarkers of tumor cell proliferation, where decreased biomarker detection after synchronous

induction of MycΔp85α in HT29 tumor xenografts acts as a first hurdle for further biomarker optimization and development.

Materials and Methods

Molecular Biology

The cDNA encoding MycΔp85α (27) was inserted into pTRE (Clontech) to generate pTREMycΔp85α. This was digested with *Ase*I (NEB) and fused with *Ase*I-linearized pN1pβactin-rtTA2^S-M2-IRES-EGFP (15) to generate pSMVMycΔp85α.

Cell Culture

HT29 cells (American Type Culture Collection) were cultured in RPMI 1640 (Life Technologies, Inc.), SW620 cells (American Type Culture Collection) in DMEM (Life Technologies), and HCT116 cells (American Type Culture Collection) and HCT116 mutant *PIK3CA* and WT *PIK3CA* (a kind gift from B. Vogelstein) in McCoy's 5A (Life Technologies), all supplemented with 10% fetal bovine serum (Biowest) in a humidified atmosphere at 37°C and 5% CO_2. Cells were routinely monitored for *Mycoplasma* and were free from infection. To generate MycΔp85α clones, cells were electroporated with 15 μg of pSMVMycΔp85α and cultured in the presence of 800 μg mL^{-1} G418 (Life Technologies) for ~2 wk. The top 10% of GFP expressing cells were then selected by fluorescence-activated cell sorting (BD FACSVantage SE); 200 cells were seeded into a 10-cm dish; and discrete colonies were picked when visible (33). MycΔp85α expression was induced by treating cells with 0.5 μg mL^{-1} dox (Clontech), and clones that expressed the lowest level of MycΔp85α while reducing the levels of phosphorylated PKB were selected for further study to minimize nonspecific protein overexpression effects. A stock solution of 10 mmol/L oxaliplatin (Alexis Biochemicals) was dissolved in PBS; a stock solution of 100 mmol/L etoposide (Sigma) was dissolved in DMSO; and a stock solution of 10 mmol/L PI-103 (Calbiochem) was dissolved in DMSO. All were diluted to the appropriate concentration in media.

Western Blotting

Cells grown *in vitro* were washed either with ice-cold PBS and lysed directly into cell lysis buffer (Cell Signaling) supplemented with Protease Inhibitor Cocktail and Phosphatase Inhibitor Cocktail I and II (Sigma), or detached and adherent cells were pooled after trypsinization and lysed in the same lysis buffer for analysis of apoptosis. Tumor xenografts were ground to a fine powder with a pestle and mortar under liquid nitrogen and lysed with the same lysis buffer. Protein concentration was determined by bicinchoninic acid assay (Thermo Scientific) following the manufacturer's instructions, and 20 μg of total protein were used per assay as previously described (15). The following primary antibodies were used: p85 (Upstate), Myc-tag (Upstate), phospho-Ser473 PKB (Cell Signaling), total PKB (Cell Signaling), p27 (Santa Cruz Biotechnology), and actin (Sigma).

Immunohistochemistry

Staining was done as previously described (34). The following primary antibodies were used: Myc-tag (Upstate), Ki67 (DAKO), and cleaved PARP (BD Pharmingen). Slides were scanned using a Zeiss Mirax Scan fitted with a 20× objective, and four images from each slide were selected at random with Mirax Viewer software. The total number of cells per slide was determined using "Nucleus Counter" plug-in for ImageJ software, and the number of positive cells in each image was counted by two independent counters.

Electrochemiluminescent Immunoassay

Detached and adherent cells were pooled after trypsinization, and the resulting cell pellets lysed for Western blotting. Twenty-five microliters of a 0.8 μg μL^{-1} lysate were analyzed in duplicate on a cleaved caspase-3 and total caspase-3 duplex electrochemiluminescent plate (Meso Scale Discovery) and analyzed on a Sector Imager 6000 (Meso Scale Discovery). Because cleaved caspase-3 and total caspase-3 levels were measured in the same well, percent cleaved caspase-3 was determined using the following formula: $(2 \times$ cleaved signal)/ (cleaved signal + total signal) $\times$ 100.

Growth Assay

Cells were seeded in 96-well plates, and 24 h later (day 0), one plate was fixed with ice-cold 10% trichloroacetic acid for 60 min and left to dry. The rest of the plates were treated with dox or dox-free medium and one plate was fixed every 24 h. Once fixed, cells were stained with 0.4% SRB for 15 min and washed with 1% acetic acid; the dye was released with 1.5 mol/L Tris-HCl (pH 8.8), and the absorbance at 540 nm read on a 96-well plate spectrophotometer.

Cell Cycle Analysis

Detached and adherent cells were harvested by trypsinization, resuspended in PBS, and fixed by adding ice-cold ethanol dropwise to a final concentration of 70% (v/v). Fixed cells were incubated with 40 μg mL^{-1} propidium iodide and 50 μg mL^{-1} RNase A in PBS for 30 min at 37°C in the dark. Propidium-bound DNA was then detected by flow cytometry (BDFacsCalibur), and the percentage of cells in each stage of the cell cycle determined using ModFit LT 3.2 modeling software (Verity Software).

Measurement of Apoptosis

Apoptotic index was calculated by counting the percent cells with apoptotic nuclear morphology. Briefly, cells were fixed as for cell cycle analysis and resuspended in Prolong Gold antifade reagent with DAPI (Invitrogen) and spotted onto a microscope slide; a minimum of 300 nuclei were analyzed on an Olympus BX51 microscope with a 100× objective lens. In addition, cells harvested by trypsinization were resuspended in Annexin Binding Buffer (BD Biosciences) and incubated with Annexin V-APC and 7-AAD (BD Bioscience) for 15 min at room temperature in the dark and analyzed on a BD FACSArray Bioanalyzer (BD Bioscience).

Tumor Xenografts

HT29 xenografts were grown by s.c. injection of 5×10^6 cells in 0.1 mL of serum-free medium into the mid-dorsal region of the back of 6- to 8-wk-old female BALB/c-nude mice (Paterson Institute for Cancer Research). Mice were housed in individually vented caging systems on a 12-h light:12-h dark environment and maintained at uniform temperature and

humidity. Tumor size was measured three times a week with calipers, and the volume calculated as (tumor length × tumor width^2)/2. When tumors reached ∼300 mm^3, animals were switched to feed containing 625 mg kg^{-1} of dox or control feed (Harlan-Teklad). On sacrifice, tumors were excised and bisected. One half was snap frozen in liquid nitrogen and used to prepare lysates and the other half was fixed in 10% formalin for immunohistochemistry. All experiments were conducted according to Home Office Regulations (UK) under Project Licence (40-2746) held by Prof. Dive.

Disclosure of Potential Conflicts of Interest

Acknowledgments

References

1. Fruman DA, Meyers RE, Cantley LC. Phosphoinositide kinases. Annu Rev Biochem 1998;67:481–507.

2. Vivanco I, Sawyers CL. The phosphatidylinositol 3-kinase AKT pathway in human cancer. Nat Rev Cancer 2002;2:489–501.

3. Huang CH, Mandelker D, Schmidt-Kittler O, et al. The structure of a human p110α/p85α complex elucidates the effects of oncogenic PI3Kα mutations. Science 2007;318:1744–8.

4. Yu J, Zhang Y, McIlroy J, Rordorf-Nikolic T, Orr GA, Backer JM. Regulation of the p85/p110 phosphatidylinositol 3′-kinase: stabilization and inhibition of the p110α catalytic subunit by the p85 regulatory subunit. Mol Cell Biol 1998;18: 1379–87.

5. Cantley LC. The phosphoinositide 3-kinase pathway. Science 2002;296: 1655–7.

6. Li J, Yen C, Liaw D, et al. PTEN, a putative protein tyrosine phosphatase gene mutated in human brain, breast, and prostate cancer. Science 1997;275: 1943–7.

7. Steck PA, Pershouse MA, Jasser SA, et al. Identification of a candidate tumour suppressor gene, MMAC1, at chromosome 10q23.3 that is mutated in multiple advanced cancers. Nat Genet 1997;15:356–62.

8. Samuels Y, Wang Z, Bardelli A, et al. High frequency of mutations of the PIK3CA gene in human cancers. Science 2004;304:554.

9. Carpten JD, Faber AL, Horn C, et al. A transforming mutation in the pleckstrin homology domain of AKT1 in cancer. Nature 2007;448:439–44.

10. Normanno N, De Luca A, Bianco C, et al. Epidermal growth factor receptor (EGFR) signaling in cancer. Gene 2006;366:2–16.

11. Rosenzweig KE, Youmell MB, Palayoor ST, Price BD. Radiosensitization of human tumor cells by the phosphatidylinositol3-kinase inhibitors wortmannin and LY294002 correlates with inhibition of DNA-dependent protein kinase and prolonged G$_2$-M delay. Clin Cancer Res 1997;3:1149–56.

12. Bain J, Plater L, Elliott M, et al. The selectivity of protein kinase inhibitors: a further update. Biochem J 2007;408:297–315.

13. Liu Y, Shreder KR, Gai W, Corral S, Ferris DK, Rosenblum JS. Wortmannin, a widely used phosphoinositide 3-kinase inhibitor, also potently inhibits mammalian polo-like kinase. Chem Biol 2005;12:99–107.

14. Holleran JL, Egorin MJ, Zuhowski EG, Parise RA, Musser SM, Pan SS. Use of high-performance liquid chromatography to characterize the rapid decomposition of wortmannin in tissue culture media. Anal Biochem 2003;323:19–25.

15. Welman A, Cawthorne C, Barraclough J, et al. Construction and characterization of multiple human colon cancer cell lines for inducibly regulated gene expression. J Cell Biochem 2005;94:1148–62.

16. Wang Q, Kim S, Wang X, Evers BM. Activation of NF-κB binding in HT-29 colon cancer cells by inhibition of phosphatidylinositol 3-kinase. Biochem Biophys Res Commun 2000;273:853–8.

17. Yeates LC, Gallegos A, Kozikowski AP, Powis G. Down-regulation of the expression of the p110, p85 and p55 subunits of phosphatidylinositol 3-kinase during colon cancer cell anchorage-independent growth. Anticancer Res 1999; 19:4171–6.

18. Ikediobi ON, Davies H, Bignell G, et al. Mutation analysis of 24 known cancer genes in the NCI-60 cell line set. Mol Cancer Ther 2006;5:2606–2612.

19. Dijkers PF, Medema RH, Pals C, et al. Forkhead transcription factor FKHR-L1 modulates cytokine-dependent transcriptional regulation of p27(KIP1). Mol Cell Biol 2000;20:9138–48.

20. Morrow CJ, Gray A, Dive C. Comparison of phosphatidylinositol-3-kinase signaling within a panel of human colorectal cancer cell lines with mutant or wild-type PIK3CA. FEBS Lett 2005;579:5123–8.

21. Samuels Y, Diaz LA, Jr., Schmidt-Kittler O, et al. Mutant PIK3CA promotes cell growth and invasion of human cancer cells. Cancer Cell 2005;7:561–73.

22. Rabik CA, Dolan ME. Molecular mechanisms of resistance and toxicity associated with platinating agents. Cancer Treat Rev 2007;33:9–23.

23. William-Faltaos S, Rouillard D, Lechat P, Bastian G. Cell-cycle arrest by oxaliplatin on cancer cells. Fundam Clin Pharmacol 2007;21:165–72.

24. Casagrande F, Bacqueville D, Pillaire MJ, et al. G$_1$ phase arrest by the phosphatidylinositol 3-kinase inhibitor LY 294002 is correlated to up-regulation of p27Kip1 and inhibition of G$_1$ CDKs in choroidal melanoma cells. FEBS Lett 1998;422:385–90.

25. Raynaud FI, Eccles S, Clarke PA, et al. Pharmacologic characterization of a potent inhibitor of class I phosphatidylinositol 3-kinases. Cancer Res 2007;67: 5840–50.

26. Weng LP, Smith WM, Dahia PL, et al. PTEN suppresses breast cancer cell growth by phosphatase activity-dependent G$_1$ arrest followed by cell death. Cancer Res 1999;59:5808–14.

27. Craddock BL, Orchiston EA, Hinton HJ, Welham MJ. Dissociation of apoptosis from proliferation, protein kinase B activation, and BAD phosphorylation in interleukin-3-mediated phosphoinositide 3-kinase signaling. J Biol Chem 1999;274:10633–40.

28. Davies SP, Reddy H, Caivano M, Cohen P. Specificity and mechanism of action of some commonly used protein kinase inhibitors. Biochem J 2000;351: 95–105.

29. Poh TW, Pervaiz S. LY294002 and LY303511 sensitize tumor cells to drug-induced apoptosis via intracellular hydrogen peroxide production independent of the phosphoinositide 3-kinase-Akt pathway. Cancer Res 2005;65:6264–74.

30. Gupta S, Ramjaun AR, Haiko P, et al. Binding of ras to phosphoinositide 3-kinase p110α is required for ras-driven tumorigenesis in mice. Cell 2007;129: 957–68.

31. Chang JG, Chen YJ, Perng LI, et al. Mutation analysis of the PTEN/MMAC1 gene in cancers of the digestive tract. Eur J Cancer 1999;35:647–51.

32. The Cancer Genome Atlas Research Network. Comprehensive genomic characterization defines human glioblastoma genes and core pathways. Nature 2008;455:1061–8.

33. Welman A, Barraclough J, Dive C. Generation of cells expressing improved doxycycline-regulated reverse transcriptional transactivator rtTA2S-M2. Nat Protoc 2006;1:803–11.

34. Barraclough J, Hodgkinson C, Hogg A, Dive C, Welman A. Increases in c-Yes expression level and activity promote motility but not proliferation of human colorectal carcinoma cells. Neoplasia 2007;9:745–54.

Molecular Cancer Research

Blocking Phosphoinositide 3-Kinase Activity in Colorectal Cancer Cells Reduces Proliferation but Does Not Increase Apoptosis Alone or in Combination with Cytotoxic Drugs

Cristina Martin-Fernandez, Juliana Bales, Cassandra Hodgkinson, et al.

Updated version	Access the most recent version of this article at: doi:10.1158/1541-7786.MCR-08-0445

Cited articles	This article cites 34 articles, 13 of which you can access for free at: http://mcr.aacrjournals.org/content/7/6/955.full#ref-list-1
Citing articles	This article has been cited by 4 HighWire-hosted articles. Access the articles at: http://mcr.aacrjournals.org/content/7/6/955.full#related-urls

E-mail alerts	Sign up to receive free email-alerts related to this article or journal.
Reprints and Subscriptions	To order reprints of this article or to subscribe to the journal, contact the AACR Publications Department at pubs@aacr.org.
Permissions	To request permission to re-use all or part of this article, use this link http://mcr.aacrjournals.org/content/7/6/955. Click on "Request Permissions" which will take you to the Copyright Clearance Center's (CCC) Rightslink site.